Supporting Information

Spontaneous Generation of Atomically Dispersed Mo and MoS_2 Coupling Catalyst by Reaction Induction Transformation for Enhancing Local Hydrogen Concentration in Hydrogenation

*Guangxun Sun,[a] Peng Xue,[a] Changle Yue,[a] Yang Li,[a] Hongfu Shi,[a] Xin Zhang,[a] Fengyu Tian,[a] Junxi Li,[a] Zekun Guan,[a] Bin Liu,[a] Zhi Liu, *[a,c] Yunqi Liu,*[a,b] Yuan Pan*[a]*

*Corresponding author: Zhi Liu, zhiliu@rcees.ac.cn; Yunqi Liu, liuyq@upc.edu.cn; Yuan Pan, panyuan@upc.edu.cn

Supplementary Text

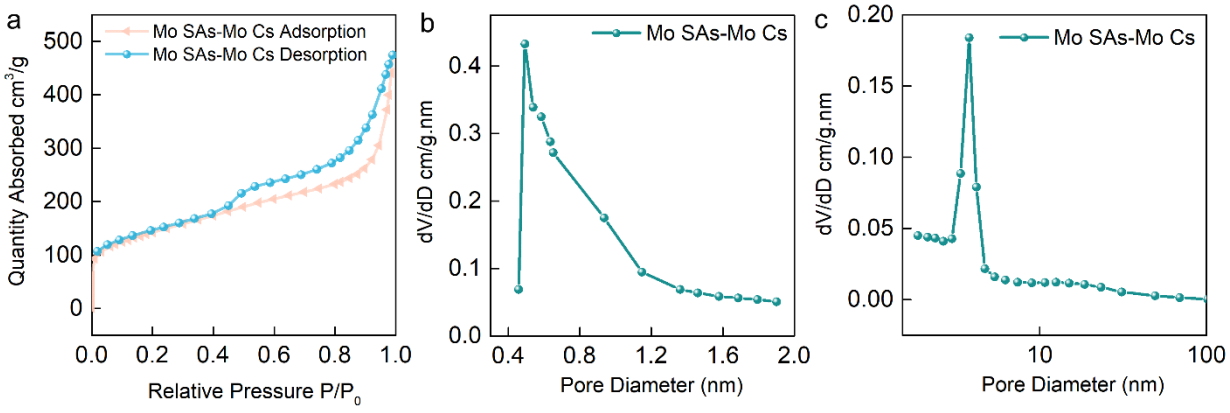

Fig. S1. (a) N_2 adsorption/desorption isotherms, (b, c) pore size distribution of Mo SAs-Mo Cs.

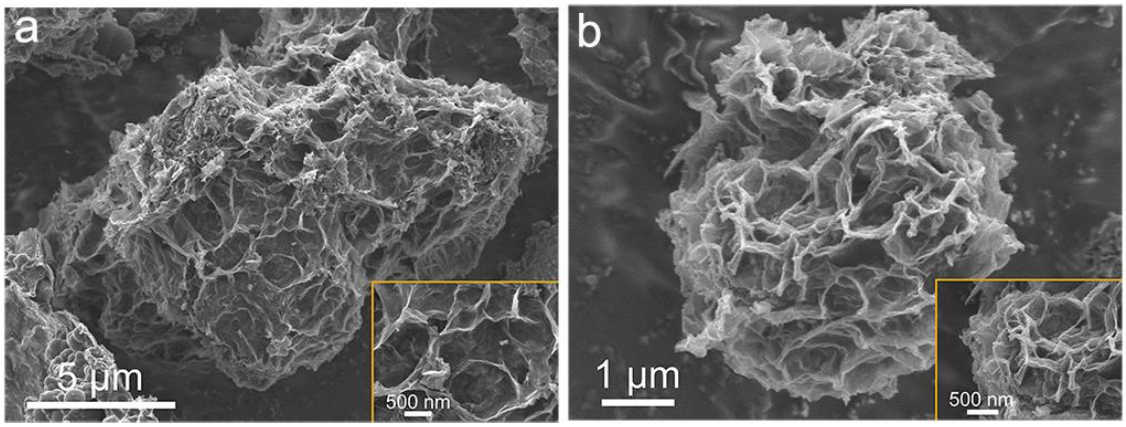

Fig. S2. (a, b) SEM image of Mo SAs-Mo Cs.

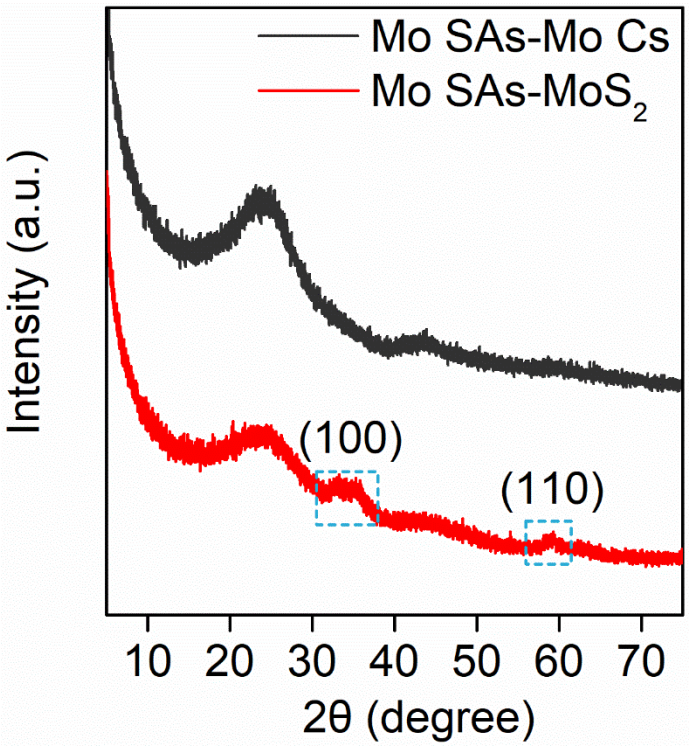

Fig. S3. XRD patterns of Mo SAs-Mo Cs and Mo SAs-MoS_2 catalysts.

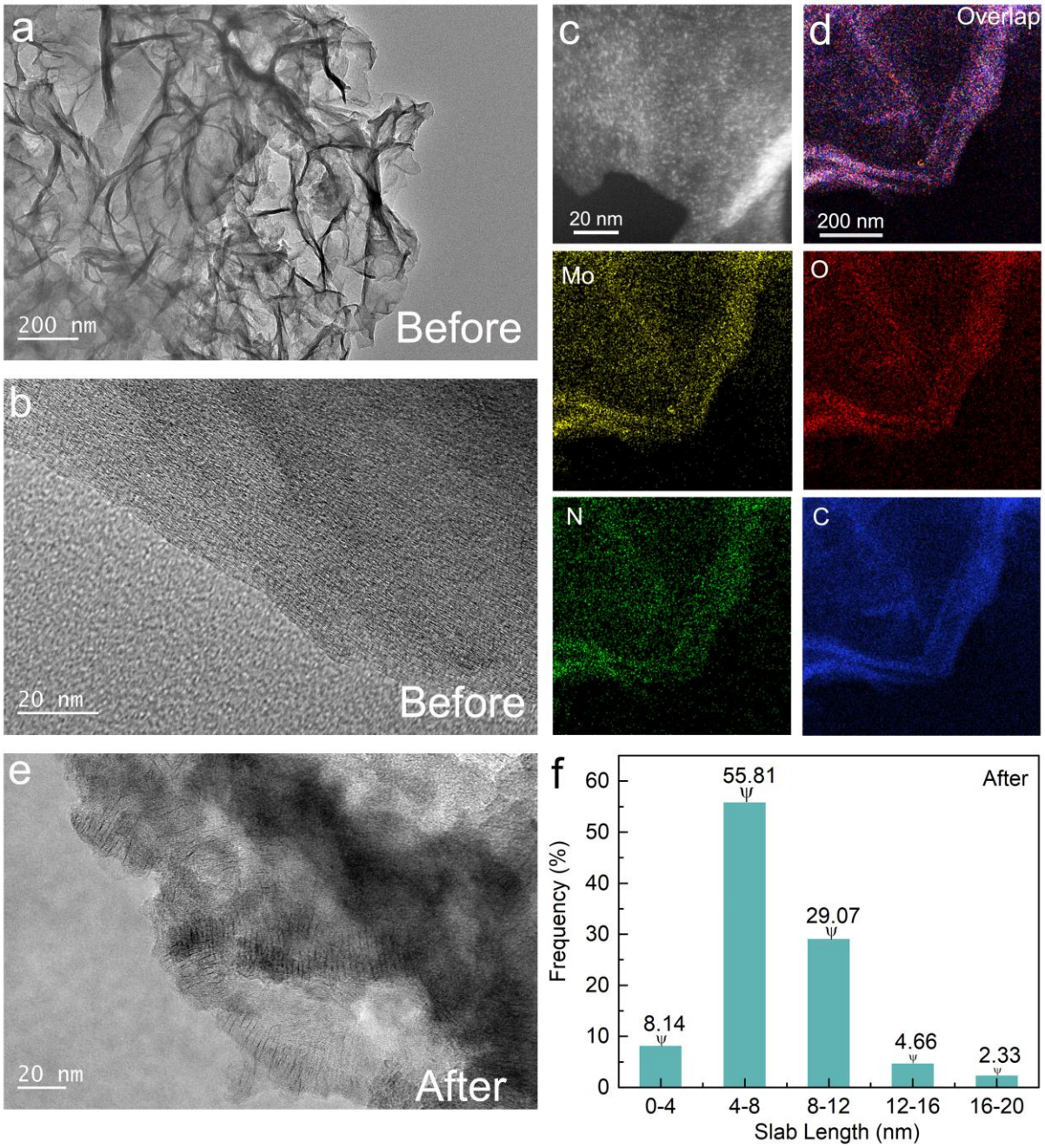

Fig. S4. Morphological of Mo SAs-Mo Cs (a) TEM. (b) HRTEM. (c) HAADF-STEM. (d) HAADF-STEM-EDS-mapping. Morphological of Mo SAs-MoS_2 (e) TEM (f) the corresponding distribution of slab length of MoS_2 nanosheets.

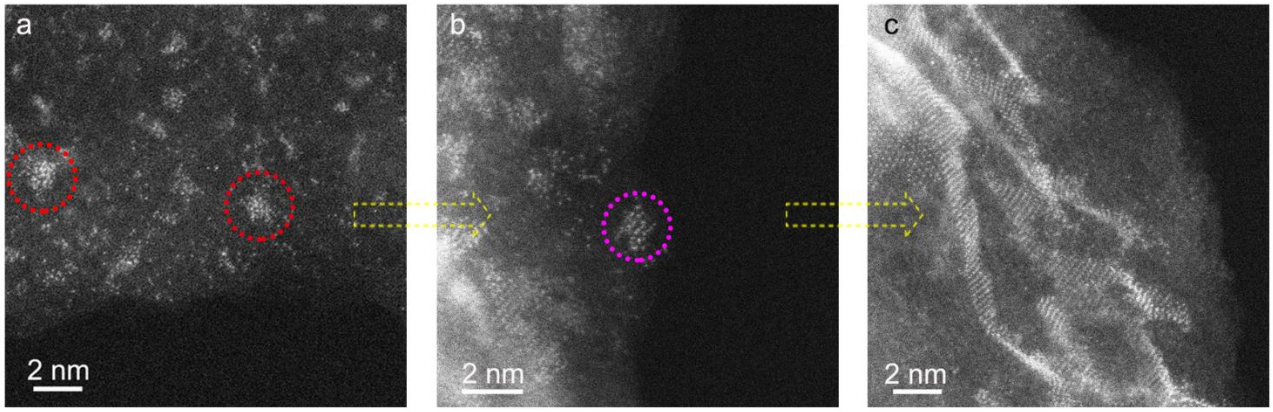

Fig. S5. AC-HAADF-STEM for the transformation of Mo clusters to MoS_2. (a) Mo SAs-Mo Cs. (b) intermediates. (c) Mo SAs-MoS_2.

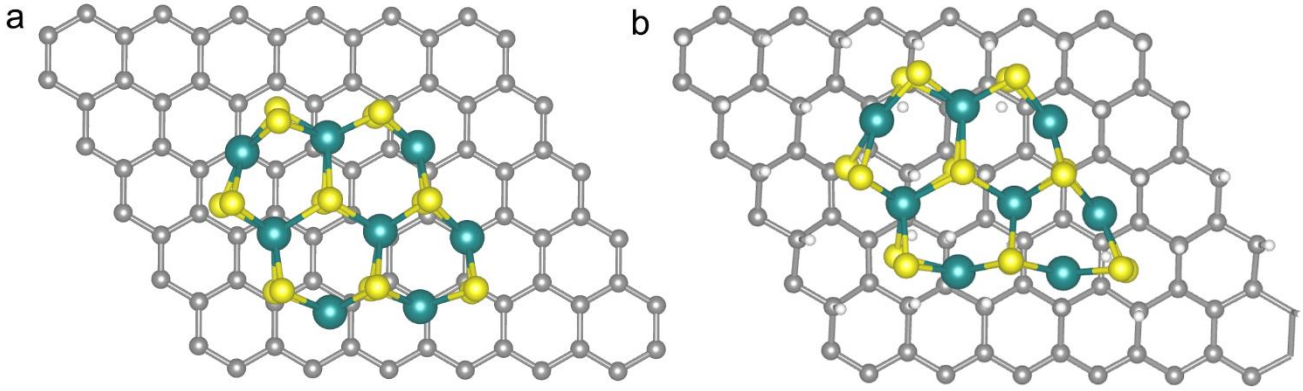

Fig. S6. The optimized configurations of (a) MoS_2 adsorption on C and (b) C-H substrate. The cyan, yellow, and grey spheres denote Mo, S, and C atom, respectively.

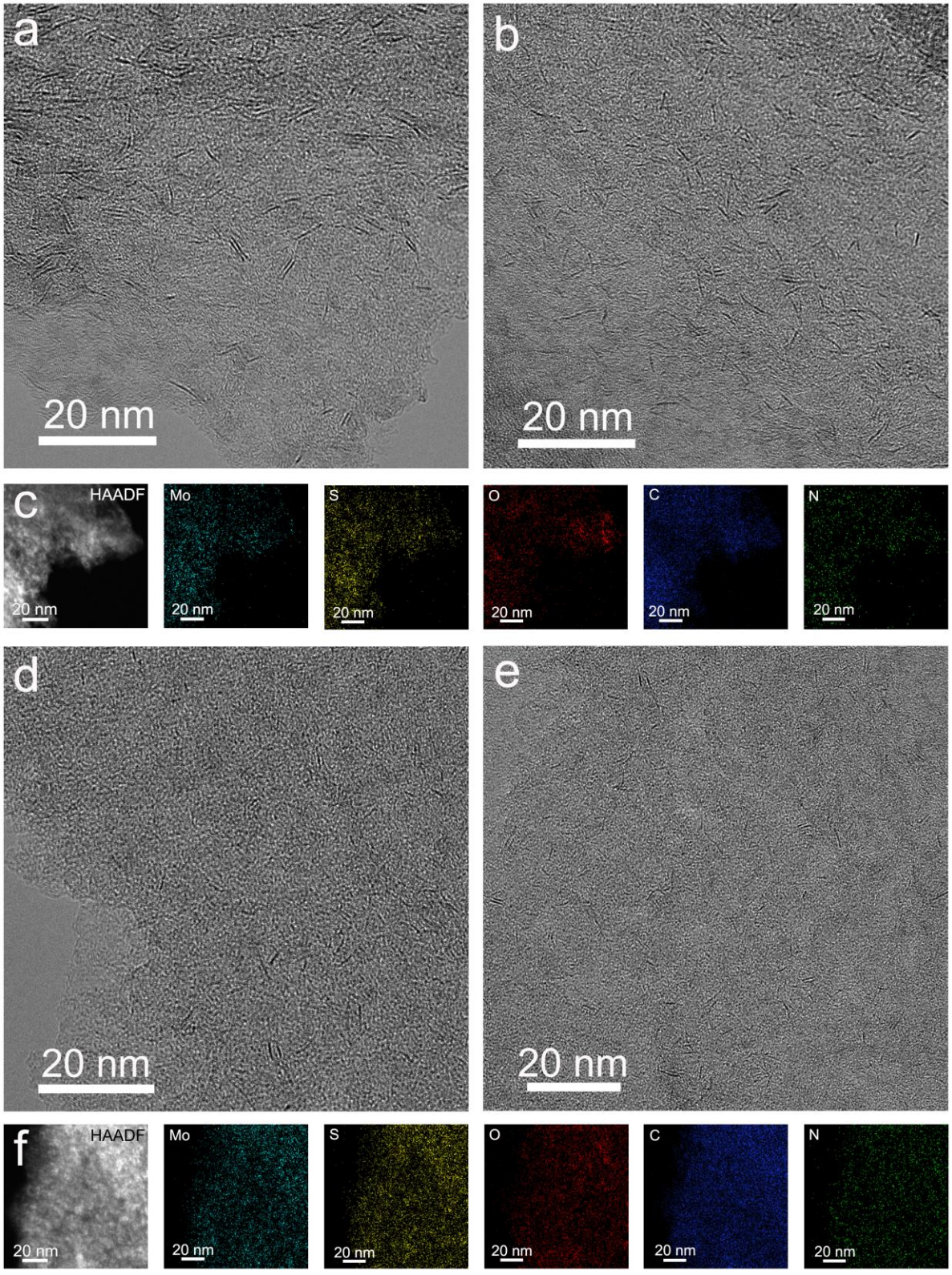

Fig. S7. Morphological of TEM images for *in situ* sulfurization of Mo species (a-c) TEM-H_2. (d-f) TEM-N_2.

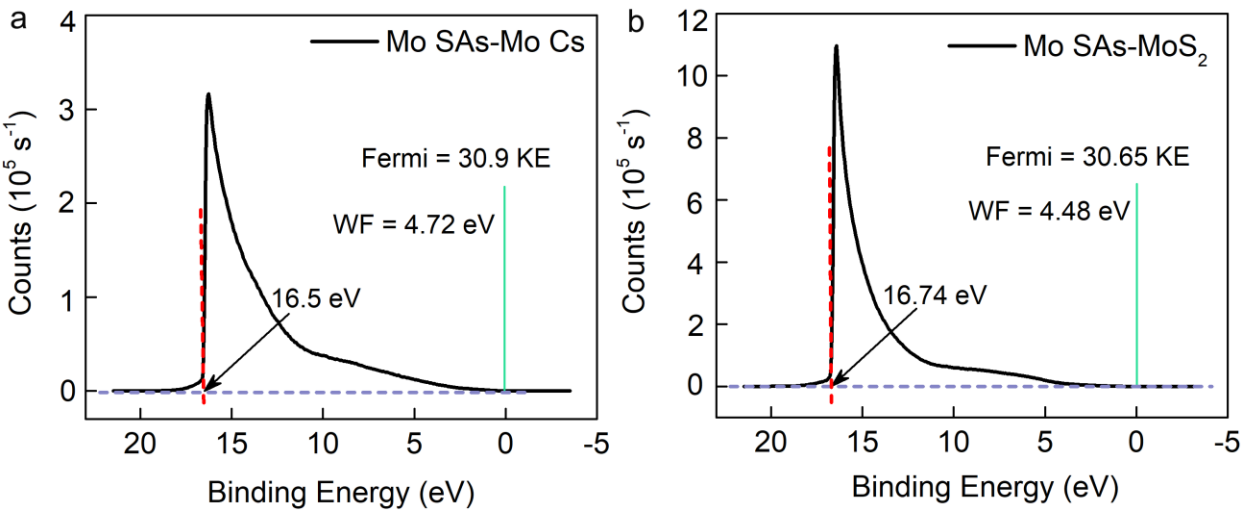

Fig. S8. UPS spectra of the catalysts before and after the reaction. (a) Mo SAs-Mo Cs, (b) Mo SAs-MoS_2.

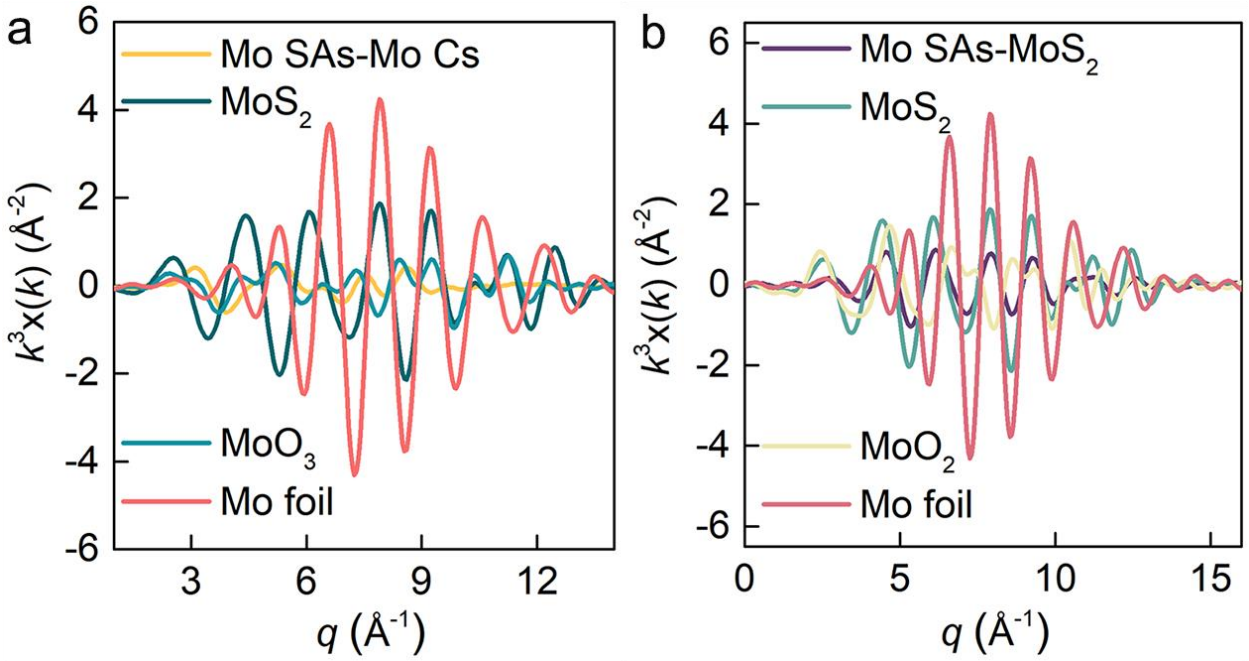

Fig. S9. EXAFS fitting curves of (a) Mo SAs-Mo Cs and (b) Mo SAs-MoS_2.

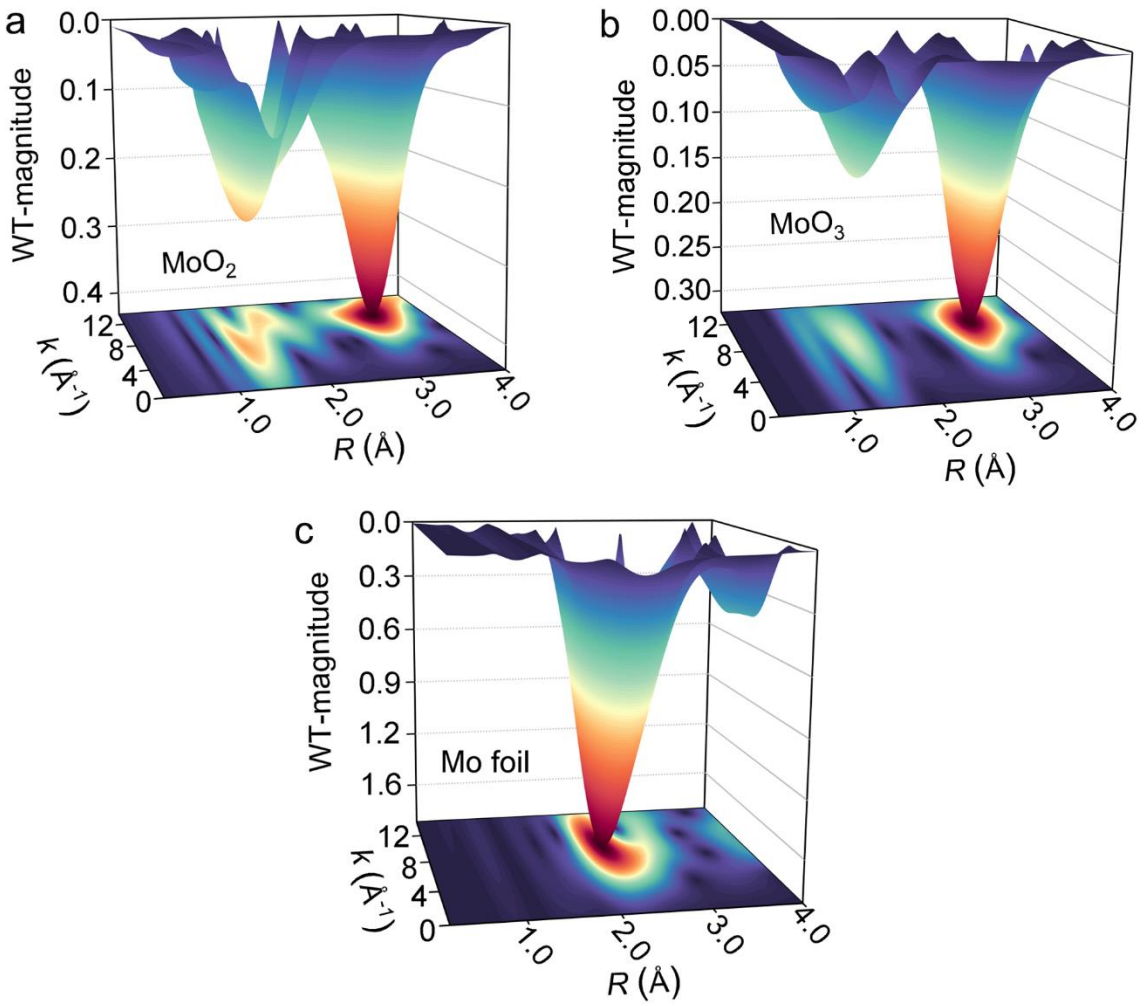

Fig. S10. WT contour plots in Mo K-edge of (a) MoO_2, (b) MoO_3 and (c) Mo foil standard.

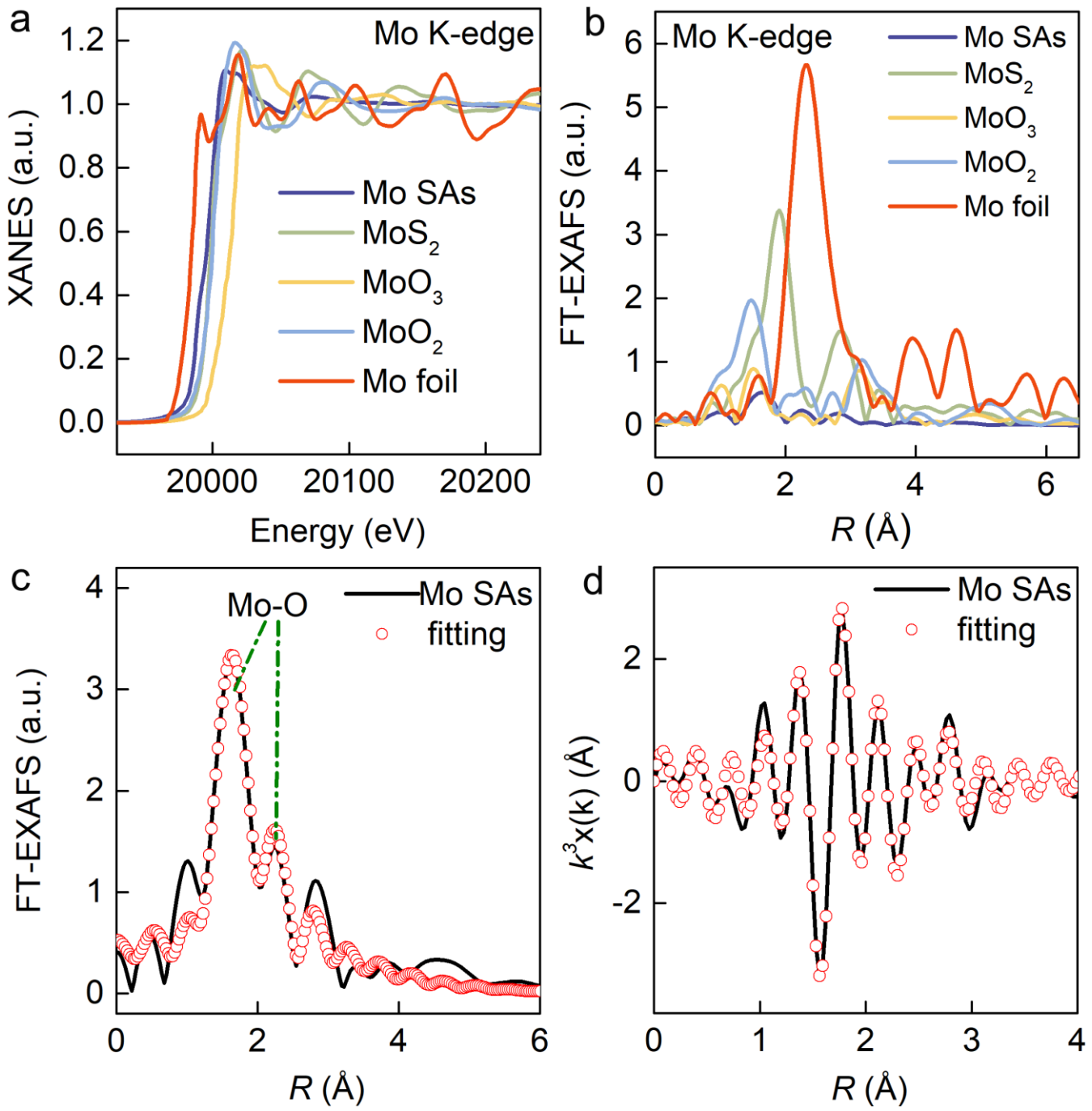

Fig. S11. Mo K-edge of Mo SAs and corresponding samples (a) XANES and (b) EXAFS. Mo K-edge EXAFS fitting curve for Mo SAs (c) FT magnitude and (d) imaginary componebt.

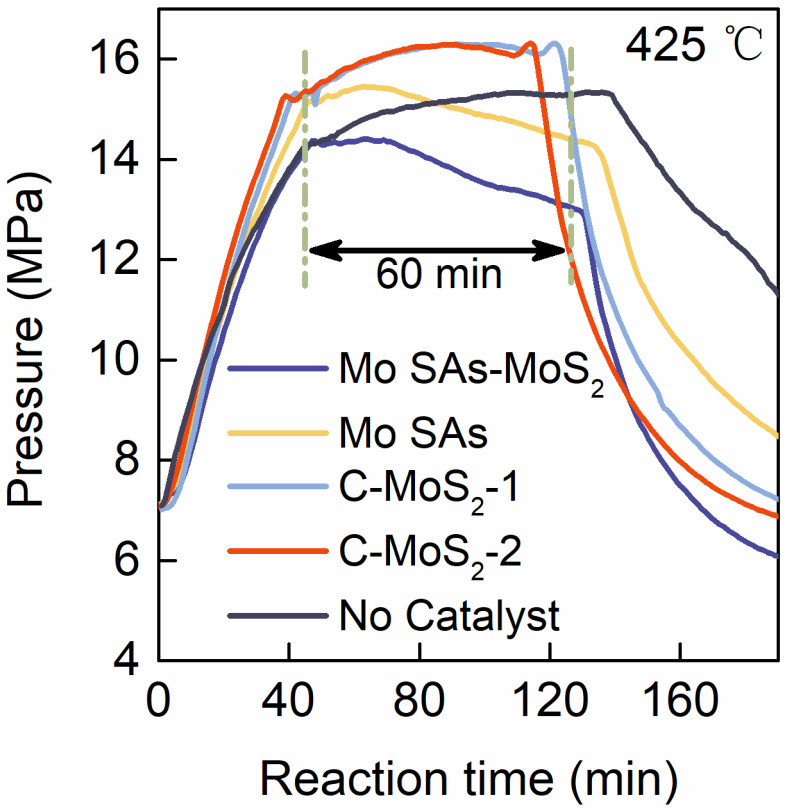

Fig. S12. H_2 consumption profiles of VR using Mo SAs-MoS_2 and corresponding catalysts at 698 K.

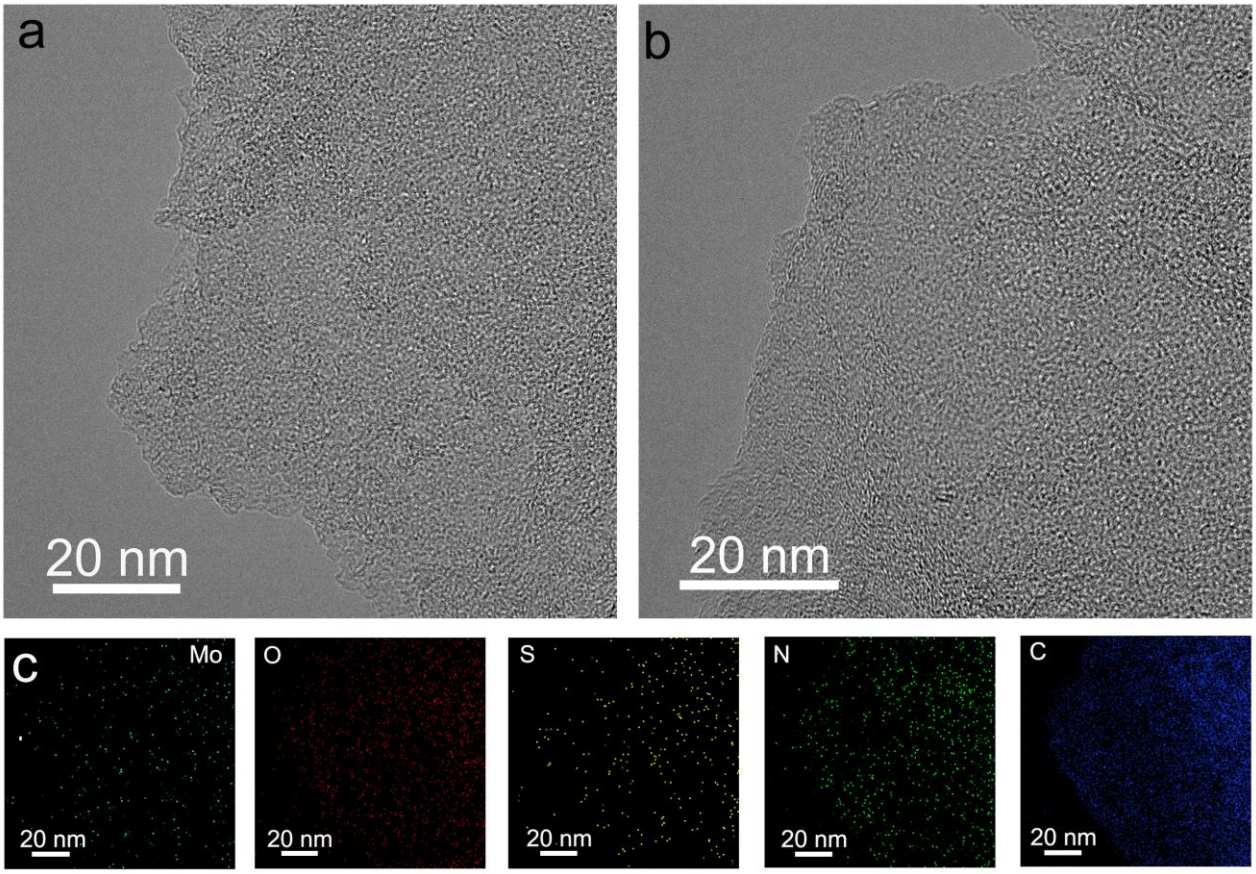

Fig. S13. Morphological of TEM images for Mo SAs before the reaction (a-b) HRTEM. (c) Mapping.

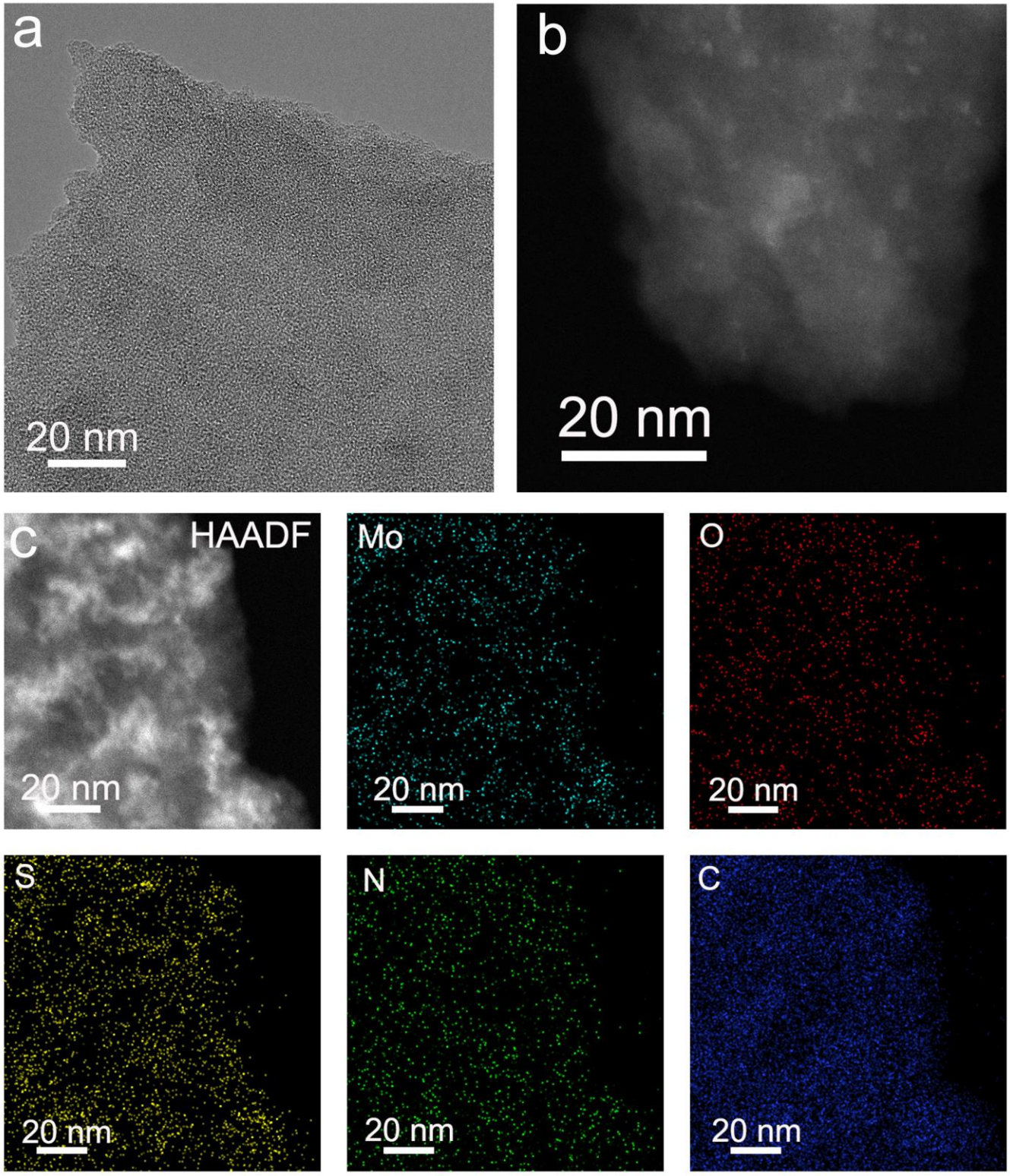

Fig. S14. Morphological of TEM images for Mo SAs after the reaction (a-b) HRTEM. (c) HAADF-STEM-mapping.

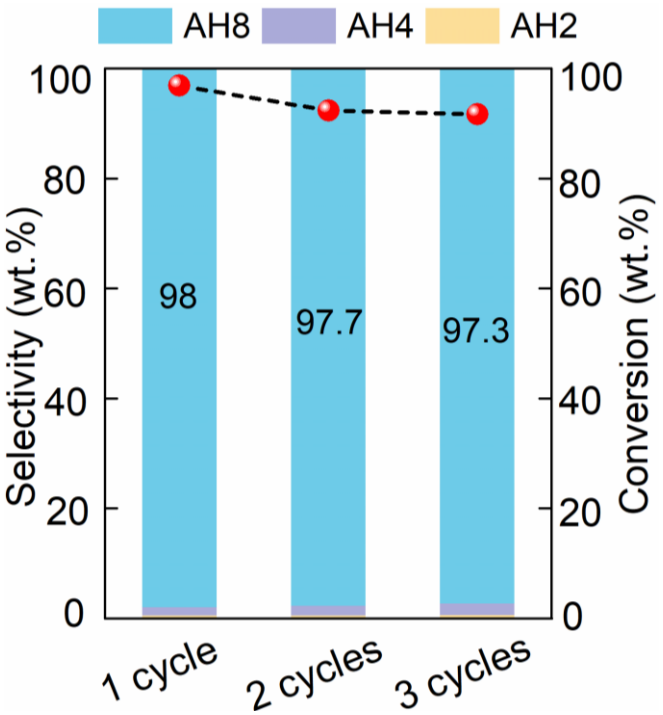

Fig. S15. Mass spectra of NH_3 in H_2 atmosphere from 100 ~ 650℃.

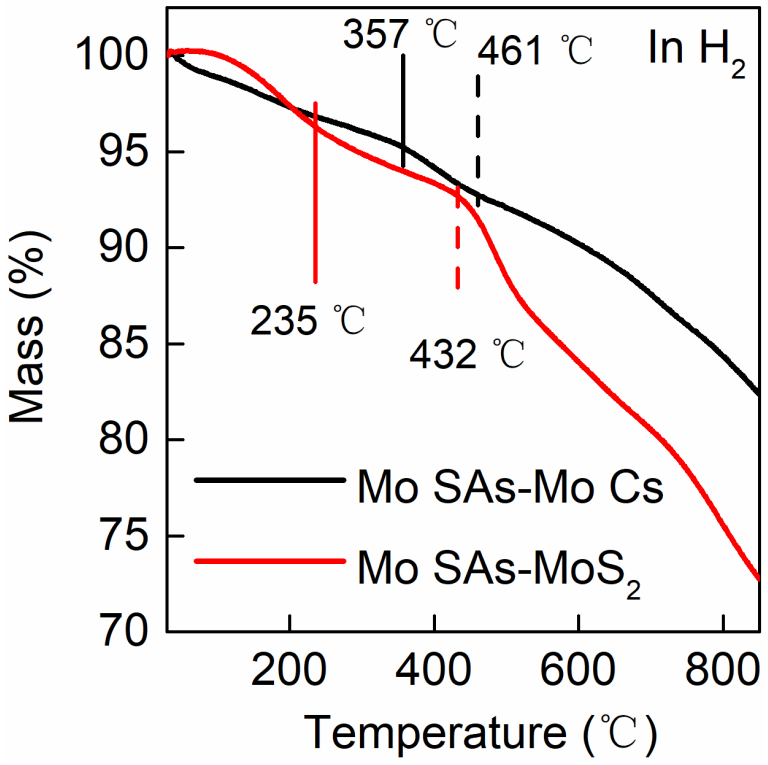

Fig. S16. Comparison of TG for Mo SAs-Mo Cs and Mo SAs-MoS_2 catalysts.

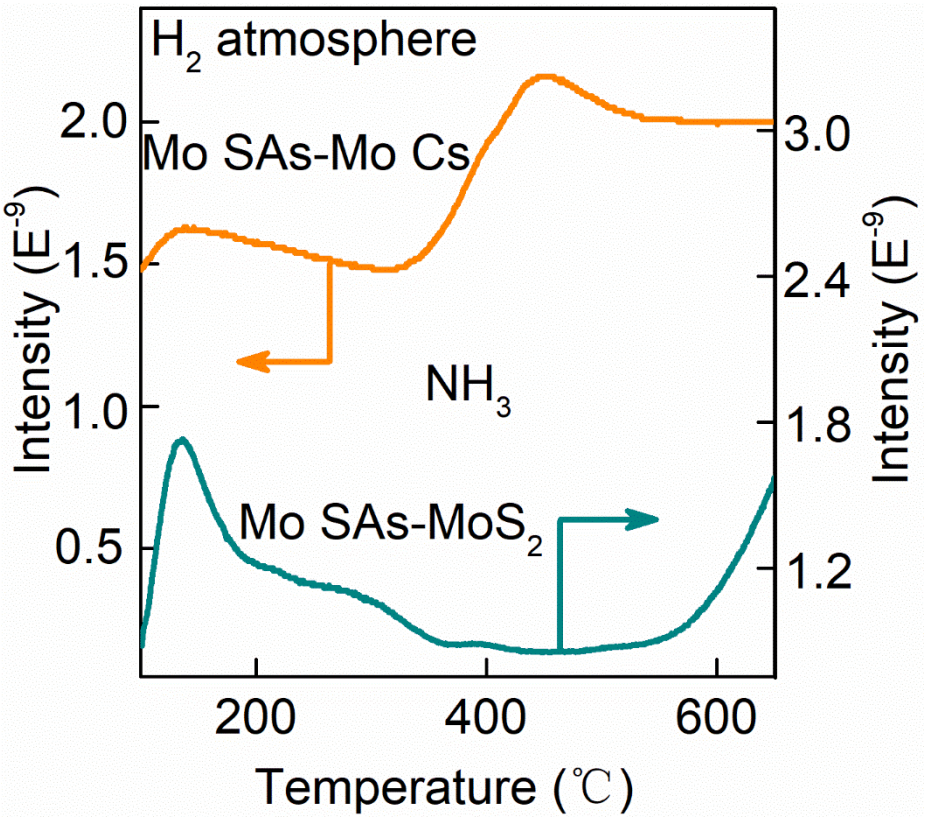

Fig. S17. Mass spectra of NH_3 in H_2 atmosphere from 100 ~ 650℃.

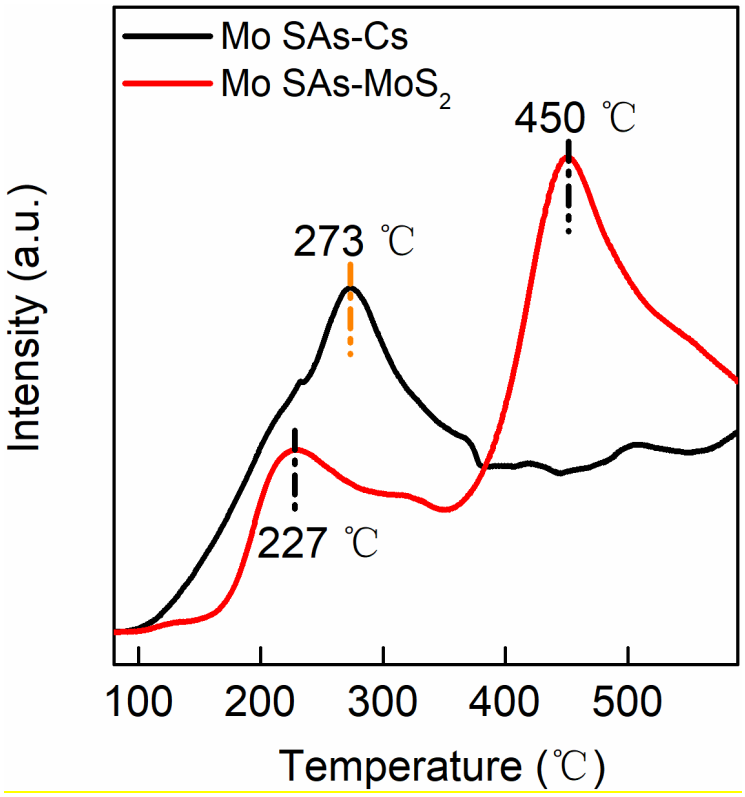

Fig. S18. H_2-TPD of Mo SAs-Cs precursor and Mo SAs-MoS_2 catalyst.

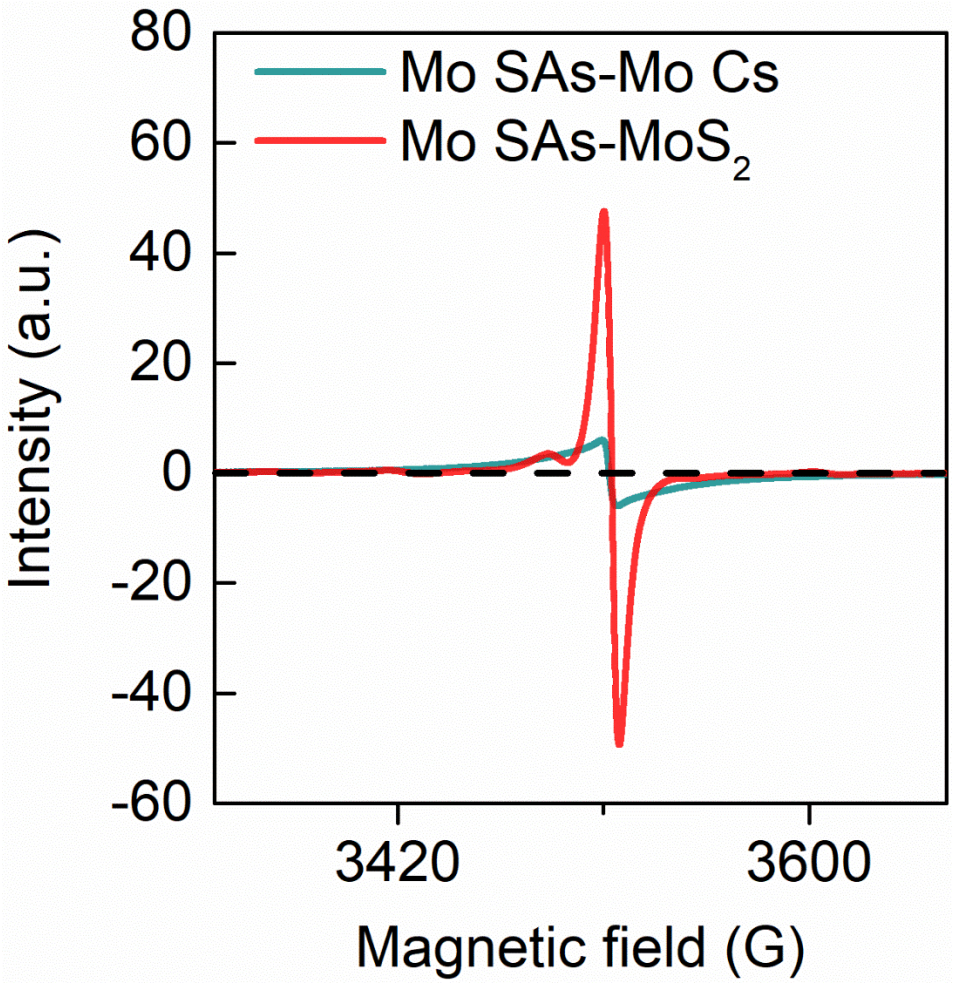

Fig. S19. EPR spectra of Mo SAs-Mo Cs and Mo SAs-MoS_2.

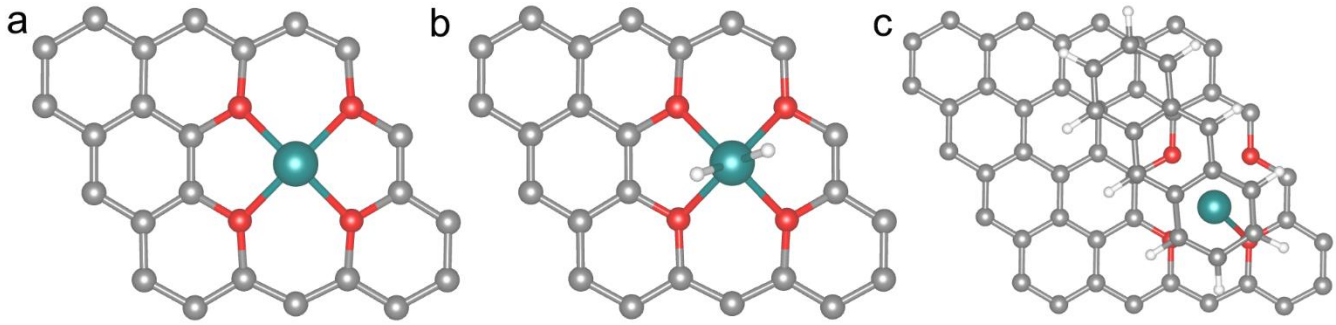

Fig. S20. The optimized configurations of (a) C-Mo, (b) C-Mo-H_2 and (c) C-Mo-AH.

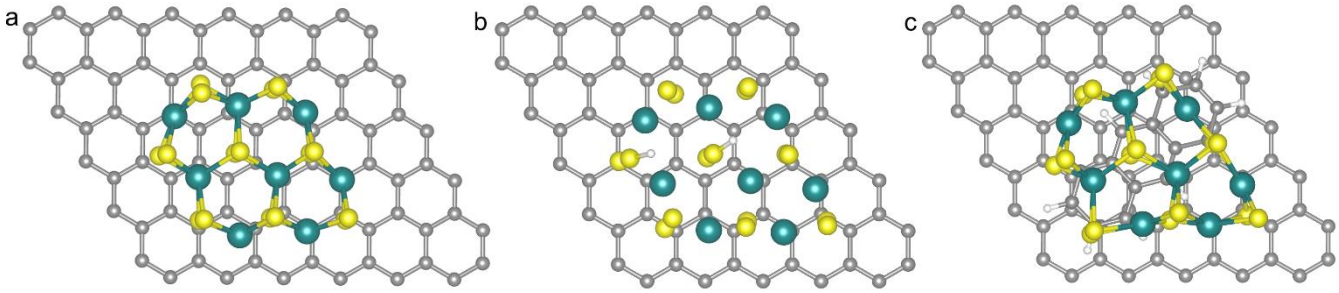

Fig. S21. The optimized configurations of (a) C-MoS_2, (b) C-MoS_2-H_2 and (c) C-MoS_2-AH.

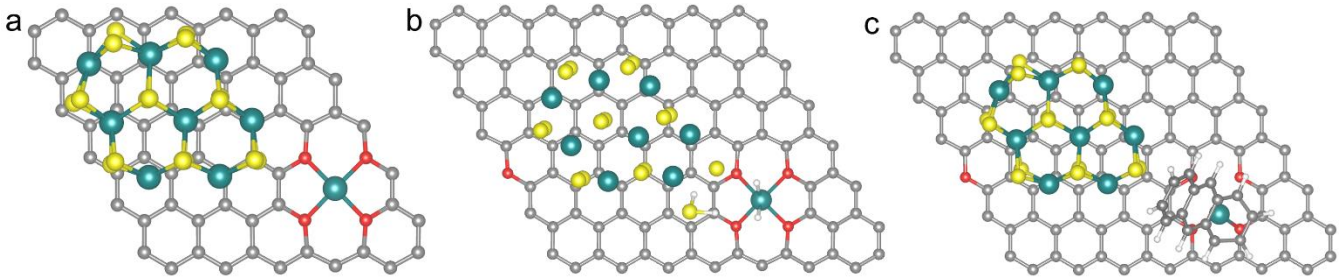

Fig. S22. The optimized configurations of (a) C-Mo-MoS_2, (b) C-Mo-MoS_2-H_2 and (c) C-Mo-MoS_2-AH.

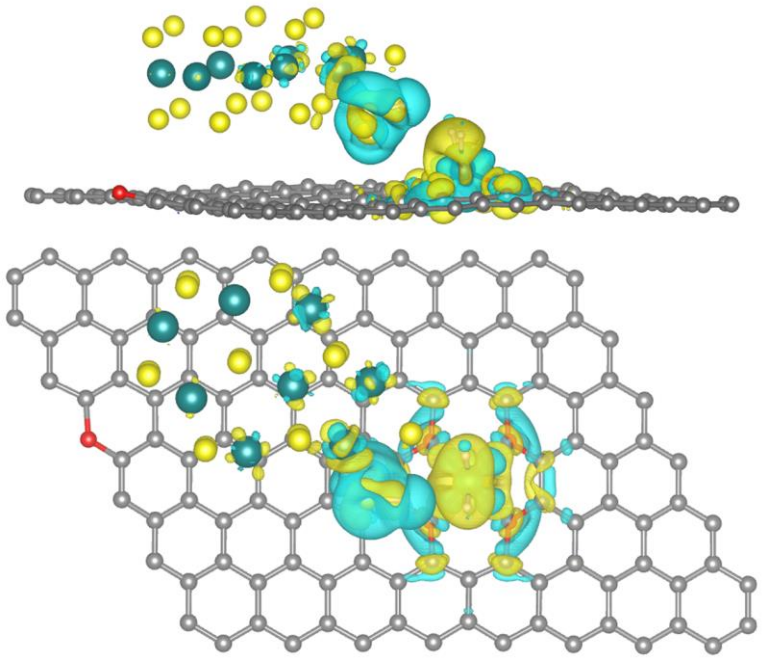

Fig. S23. Charge density of anthracene adsorption in C-Mo, C-MoS_2, C-Mo-MoS_2.

Table S1. The specific components of VR.

VR	Amount
Density (20℃) ($g \cdot cm^{-3}$)	1.039
S (wt.%)	5.2
N (wt.%)	0.56
Carbon residue (wt.%)	27.03
Ni ($\mu g \cdot g^{-1}$)	73.6
V ($\mu g \cdot g^{-1}$)	204
Fe ($\mu g \cdot g^{-1}$)	74.7
Ca ($\mu g \cdot g^{-1}$)	88
Resins (wt.%)	25.78
C7-Asphaltene (wt.%)	15.19
Saturates (wt.%)	12.18
Aromatic (wt.%)	46.59
H/C (atomic)	1.45

Table S2. Structural parameters of Mo SAs-Mo Cs, Mo SAs-MoS_2, and Mo SAs samples extracted from the EXAFS fitting.

Sample	Scatter-ing pair	CN	R(Å)	σ^2(10^{-3}Å^2)	ΔE_0(eV)	R
Mo SAs-Mo Cs	Mo-O	3.95	1.56 (1)	0.001	10 (7)	0.01
	Mo-Mo	6.22	3.01 (1)	0.004		
Mo SAs-MoS_2	Mo-O	4.41	1.97 (4)	0.002	7.3 (2)	0.01
	Mo-S	1.73	2.43 (1)	0.003		
Mo SAs	Mo-O	3.62	2.16 (3)	0.004	4.8 (2)	0.02

S_0^2 is the amplitude reduction factor S_0^2=1.0; CN is the coordination number; R is interatomic distance (the bond length between central atoms and surrounding coordination atoms); σ^2 is Debye-Waller factor (a measure of thermal and static disorder in absorber-scatterer distances); ΔE_0 is edge-energy shift (the difference between the zero kinetic energy value of the sample and that of the theoretical model). R factor is used to value the goodness of the fitting.

Table S3. Comparison of hydrogenation performance of Mo SAs-MoS_2 catalysts with various reported catalysts.

Catalyst	Quanti-ties ppm	Temperature ℃	Initial pres-sure MPa	Time h	Coke wt.%	TOF_T s^{-1}	Anthra-cene Conver-sion wt.%	Ref.
Mo SAs-MoS_2	200	425	7	1	0.6	0.39	99.4	This work
Fe-MoS_2	2000	425	9	2	1.7	-	-	Fuel. 2024, 374, 132465
NiMo	500	425	7	1	0.9	0.36	98.8	Chem. Eng. J. 2024, 498, 155166
Fe-O-B_{24}	30000	440	13	4	2.0	-	-	Fuel. **2023**, 332, 126063.
Mo SAs/C	200	425	7	1	0.63	0.35	-	Sci. Bull. **2023,** 68, 503-515.
$CoWS_2$	150	420	7	2	1.3	0.76	-	J Catal. **2023**, 421, 145-155.
Mo/ASA	-	430	11	3	0.5	-	-	Pet. Sci. **2023**, 20, 2575-2584.

Mo-A/R	150	430	7	1	0.5	1.15	-	Chem. Eng. Res. Des. **2022**, 321, 124029.
$FeNiS_x$	500	430	7	1	1.4	-	-	Fuel. **2022**, 321, 124029.
$[N_x]_2MoO_4$	-	430	12.3	3	1.1	0.21	-	Chem. Eng. Sci. **2022**, 253, 117516.
MoS_2-ES	360	400	5	4	3.2	0.089	-	J. Catal. **2019**, 369, 111-121.
MoS_2	2000	410	8	1	1.84	-		